

CARMENES in SPIE 2014. Building a fiber link for CARMENES

J. Stürmer^a, O. Stahl^a, C. Schwab^f, W. Seifert^a, A. Quirrenbach^a, P.J. Amado^e, I. Ribas^a, A. Reiners^c and J.A. Caballero^d

^aZAH-Landessternwarte Heidelberg, Königstuhl 12, 69117 Heidelberg, Germany; ^bInstitut de Ciències de l'Espai (IEEC-CSIC), Campus UAB, Facultat de Ciències, Torre C5-parell, 2a pl., E-08193 Bellaterra, Spain; ^cInstitut für Astrophysik (IAG), Friedrich-Hund Platz 1, D-37077 Göttingen, Germany; ^dCentro de Astrobiología (CSIC-INTA), Campus ESAC, PO Box 78, E-28691 Villanueva de la Cañada, Madrid, Spain; ^eInstituto de Astrofísica de Andalucía (CSIC), Glorieta de la Astronomía s/n E-18008 Granada, Spain; ^fSagan Fellow, Department of Astronomy & Astrophysics Pennsylvania State University, 525 Davey Lab University Park, PA-16802, USA

ABSTRACT

Optical fibers have successfully been used to couple high-resolution spectrographs to telescopes for many years. As they allow the instrument to be placed in a stable and isolated location, they decouple the spectrograph from environmental influences. Fibers also provide a substantial increase in stability of the input illumination of the spectrograph, which makes them a key optical element of the two high-resolution spectrographs of CARMENES. The optical properties of appropriate fibers are investigated, especially their scrambling and focal ratio degradation (FRD) behaviour. In the laboratory the output illumination of various fibers is characterized and different methods to increase the scrambling of the fiber link are tested and compared. In particular, a combination of fibers with different core shapes shows a very good scrambling performance. The near-field (NF) shows an extremely low sensitivity to the exact coupling conditions of the fiber. However, small changes in the far-field (FF) can still be seen. Related optical simulations of the stability performance of the two spectrographs are presented. The simulations focus on the influence of the non-perfect illumination stabilization in the far-field of the fiber on the radial velocity stability of the spectrographs. Using their ZEMAX model it is simulated how the barycentres of the spots move depending on the FF illumination pattern and therefore how the radial velocity is affected by a variation of the spectrograph illumination. This method allows to establish a quantitative link between the results of the measurements of the optical properties of fibers on the one hand and the radial velocity precision on the other. The results provide a strong indication that 1 m s^{-1} precision can be reached even without the use of an optical double scrambler, which has successfully been used in other high-resolution spectrographs. Given the typical throughput of an optical double scrambler of about 75 % to 85 %, our solution allows for a substantially higher throughput of the system.

Keywords: High-resolution spectroscopy, optical fiber, scrambling, FRD, modal noise

1. INTRODUCTION

In the last decades the long-term stability and relative radial velocity precision of high-resolution spectrographs has been increased enormously. Modern spectrographs like HARPS can measure radial velocities with a precision of better than 1 m s^{-1} blabla. This has only been possible by using optical fibers, which decouple the spectrograph from the varying environmental conditions of the telescope, like temperature, pressure and telescope position. Furthermore, fibers provide a stabilization and homogenization of the input illumination of a spectrograph. Most spectrographs image their input slit onto the detector, which is - in the case of a fiber-fed instrument - an image of the fiber itself. Changes in the illumination of the fiber output might transfer into a shift or at least in a change of the shape of spectral lines. Therefore it is desirable to stabilize the output of the fiber even further,

Send correspondence to J. Stürmer - E-mail: j.stuermer@lsw.uni-heidelberg.de

which has been done in the past by implementing additional optics and/or by using fibers with non-circular core cross sections (see Bouchy et al., 2013). Changes in the barycentre in the image plane of a fiber can more or less directly be translated into shifts of the spectral lines. Apart from this effect there is another illumination effect that has poorly been quantified in the past, which is the change of illumination within the pupil plane of the fiber and its effects on the stability of spectrographs. This work gives a summary of the fiber related research which has been done during designing the fiber link for CARMENES. The aim was to design a system that provides sufficient stabilization for reaching 1 m s^{-1} precision, while keeping the throughput as high as possible.

2. CARMENES

CARMENES is a high-resolution spectroscopy project for the 3.5 m telescope at the Calar Alto Observatory, consisting of two $R \sim 82000$ echelle spectrographs, one for the visual range from 550 nm to 950 nm (VIS) and one for the near infrared range from 950 nm to 1700 nm (NIR). The main scientific goal of CARMENES is to look for planets within the habitable zones of 300 low-mass stars. The advantage of CARMENES is that visual as well as near infrared spectra can be taken at the same time, which helps to distinguish wavelength dependent stellar activity effects from real planetary signals. In order to detect earth-size planets, CARMENES needs to be able to measure radial velocities with a precision better than 3 m s^{-1} . CARMENES aims for 1 m s^{-1} RV precision. At this level of precision the illumination stabilization provided by optical fibers is essential.

As shown in Fig. 1, CARMENES uses 14 fibers in total for different purposes. For each channel large core fibers ($D=400 \mu\text{m}$) are guiding calibration light from the two Calibration Units (CU) towards the front-end (FE) at the telescope. The light from the target stars is split up into its visual and near-infrared components directly in the FE. In each wavelength range the starlight as well as the calibration light is fed into two $100 \mu\text{m}$ circular fibers with a length of 42 m (VIS) / 50 m (NIR) each. One fiber is illuminated by starlight, another one by calibration light. For both the VIS and the NIR channel, the same type of fiber with a low concentration of hydroxyl groups is used (CeramOptec WF), which provides high internal throughput within the whole spectral range of both instruments. Before entering the vacuum tank of each spectrograph, the circular fibers are linked to fibers with an octagonal core with a size of $100 \mu\text{m}$ by an FC-FC junction.

For each channel a large core fiber is used to guide light collected from the 0^{th} order of the echelle grating towards a photon counter to provide information on the exposure.

The fiber link of CARMENES is currently under construction. The $100 \mu\text{m}$ fibers and their vacuum feedthroughs are assembled inhouse. Almost all interfaces use FC-connectors with ceramic ferrules as they have tighter tolerances on their inner diameters as well as better concentricities compared to metal ferrules or standard SMA connectors. The prototype of the FC-FC junction had a throughput of $\sim 94\%$ due to loose connector tolerances. It is expected that the light loss of the final junction is well below 5% .

3. SCRAMBLING AND FRD MEASUREMENTS

For any fiber coupled spectrograph the light from the star/object can only be fed to the fiber with a limited precision and repeatability. Errors of the guiding of the telescope, different focus positions, seeing variations and other environmental parameters (e.g. temperature) all lead to a change of the exact coupling conditions of the fiber. Luckily while the light is travelling along the fiber, part of this spatial information is lost. This important property of a fiber is called scrambling and is one of the biggest benefits of a fiber fed spectrograph compared to a slit spectrograph. But fibers do not make the output fully independent of their inputs, therefore changes in the fiber illumination result in a varying fiber output. This can, in the case of an echelle spectrograph, easily be misinterpreted as a change of the spectral content of the light.

A second important property of optical fibers is that they do not conserve the étendue i.e. fibers tend to scatter light into a cone which is larger than the cone of the incoming light. This effect is often called focal ratio degradation. Haynes et al. (2011) describe in detail how different physical processes contribute to FRD. However, in practise FRD is mostly dominated by connectorization effects and additional artificial FRD due to slight misalignments of the optical axis of the fiber and the rest of the optical system (see Avila, 1988). Scrambling and FRD are therefore important quantities for high-resolution spectrographs which need to be understood and tested when designing a fiber link. In the next section the optical setup of our fiber testbench is described in detail, as reliable and reproducible results strongly depend on a correct setup.

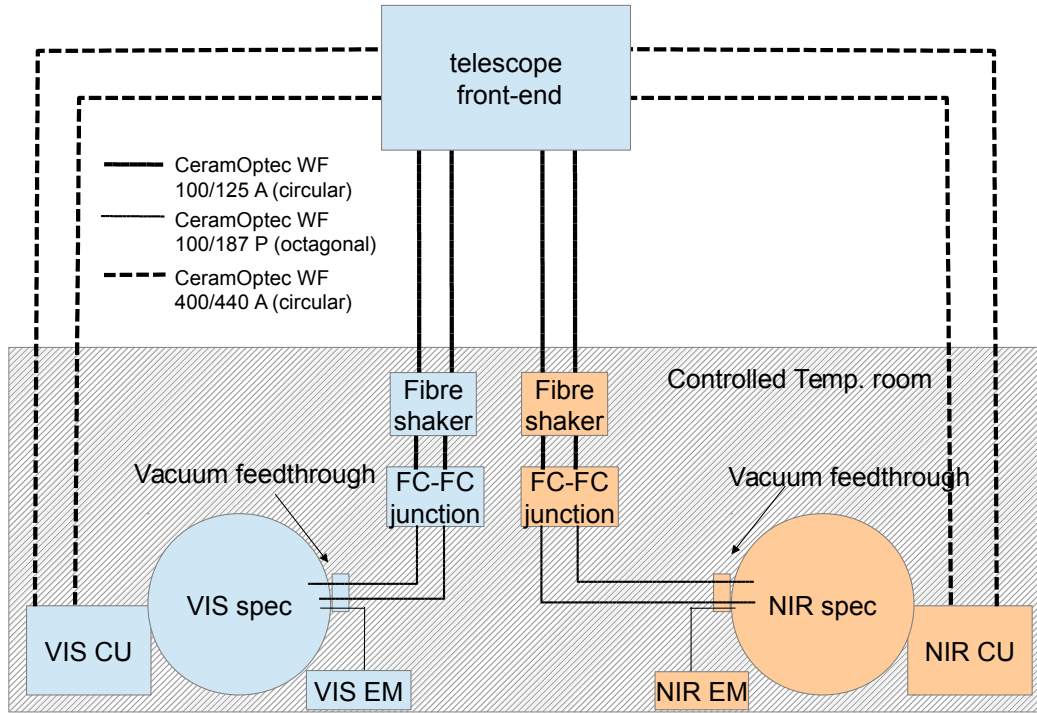


Figure 1. Fibers used in CARMENES. The total length of the fibers carrying the light from the calibration units (CU) to the front-end is 60 m, the actual science fibers consist of a 42 m (VIS) / 50 m (NIR) circular fiber and another ~ 8 m octagonal fiber, connected by an FC-FC junction.

3.1 Optical setup

The basic purpose of the setup is to measure FRD and scrambling by re-imaging a polychromatic source onto a fiber investigating its output. If not stated otherwise a white LED with a spectral peak around 450 nm was used as the light source. The LED is re-imaged onto a pinhole, while two diffuser plates help to provide homogeneous illumination of the pinhole. The pinhole itself is re-imaged again onto the fiber under investigation. An aperture stop is used to set the exact F-ratio of the beam which feeds the fiber (see Fig. 2). For scrambling tests a $10\ \mu\text{m}$ pinhole is used, while for testing the FRD a $50\ \mu\text{m}$ pinhole is put in. The pinhole is imaged 1 : 1 onto a fiber, which is mounted on an XYZ stage and a gimbal mount for tip/tilt adjustments. The Y-axis is motorized. A beamsplitter in the collimated beam allows the fiber input to be directly imaged with a camera. By doing so, one can precisely determine where the spot hits the fiber.

In the near-field setup the output of the fiber is re-imaged by a $20\times$ microscope lens to a small b/w CMOS camera, which allows for a good sampling of the near-field: A $100\ \mu\text{m}$ fiber is re-imaged to a disk with ~ 400 pixel diameter (see lower left of Fig.2).

For investigating the far-field, the fiber is mounted in front of a large CCD chip without additional optics. A cooled FLI 16803 CCD Camera with $4\text{k}\times 4\text{k}$ pixels is used. See lower right of Fig.2. The FLI Focuser attached to the CCD is used to move the CCD in the Z direction remotely by well defined steps, for FRD measurements. Although the setup does not allow one to look at the near- and the far-field simultaneously, it only takes seconds to switch between the two setups. Because the FC-connector tips always settle at the same axial distance, the reproducibility is very good.

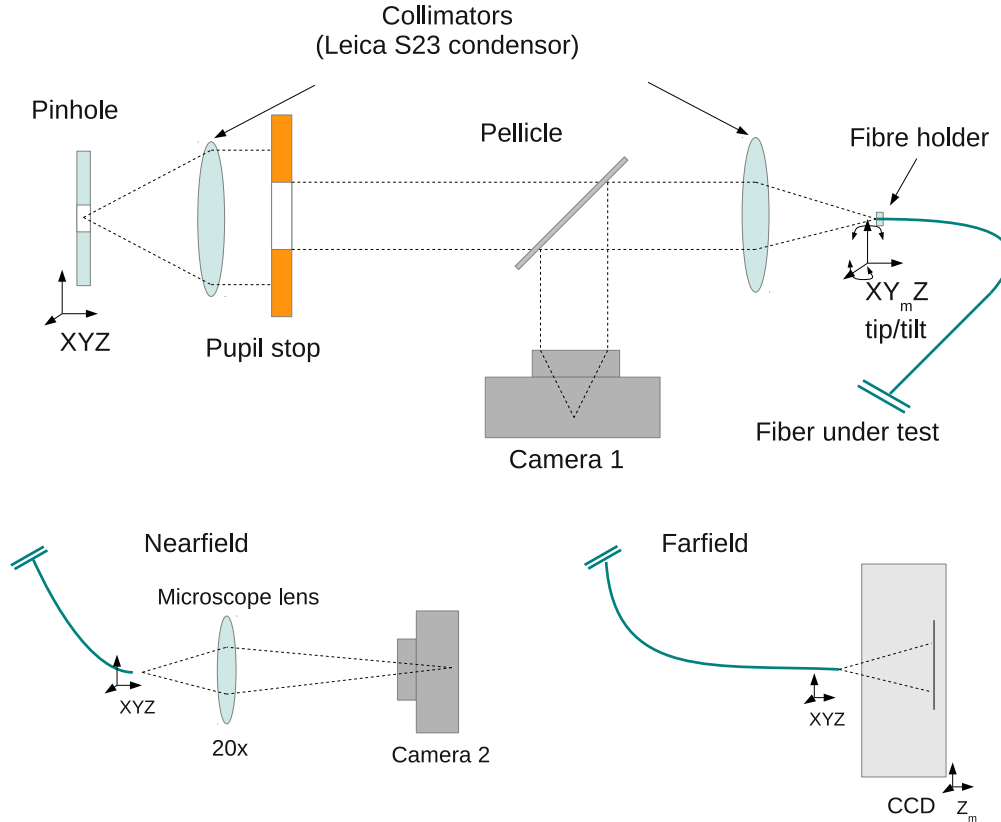


Figure 2. Setup to measure near- and far-field

3.2 FRD measurements

For measuring the FRD the angle of the cone of light exiting the fiber has to be determined. Since the exact distance between the CCD and the fiber is unknown at the beginning, a differential method is used. The F-ratio of the outgoing beam is calculated using a linear fit to the spot sizes at different distances between the detector and the fiber. In an automated procedure, three images each at five different positions are taken. After dark subtraction the size of the spot is determined by calculating the radius of 95% encircled energy (EE95). As mentioned above, FRD measurements can easily be contaminated by misalignment of the optical axis of the fiber with respect to the illumination system. In order to avoid this effect the tip/tilt angle is adjusted at the beginning of the procedure until the spot size is minimized at a fixed distance of the fiber to the CCD, as suggested by Murphy et al. (2008). Other error contributions to FRD measurements are non-perfect collimation, errors in the aperture stop diameter and deviations from a top-hat profile of the pupil illumination. It should also be noted that the calculated FRD value also depends on the encircled energy level used for the determination of the spot size. Choosing EE99 or EE90 will lead to slightly different results (see Wang et al., 2013). This makes the comparison of absolute numbers with values given in the literature very difficult.

3.3 Scrambling gain measurements

To measure the scrambling gain a series of images of the NF is made for different positions of the spot on the entrance of the fiber. The spot is displaced across the fiber entrance by a motorized axis of the XYZ-stage. Usually in literature the scrambling gain is defined as the ratio of the relative displacement of the barycenter at

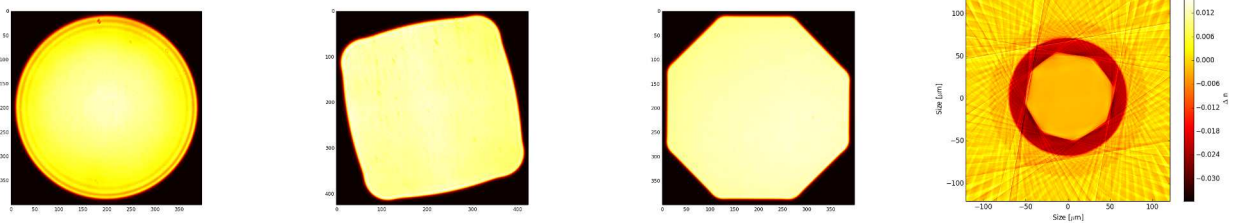


Figure 3. Near-field images of different fibers. Circular, square and octagonal fibers with $100\ \mu\text{m}$ are shown here. At the far right a measurement of the refractive index of the octagonal fiber is shown. The octagonal core is surrounded by a circular cladding with a lower refractive index, followed by another circular cladding with a refractive index similar to that of the core. The stripes are residuals from the measuring procedure.

the entrance d_i/D_i and the relative displacement of the barycenter at the output d_o/D_o :

$$SG = \frac{d_i/D_i}{d_o/D_o} \quad , \quad (1)$$

however, this definition is somewhat problematic. First, in general this number is not a constant for different spatial displacements d_i , thus it is always more conclusive to look at a series of displacements rather than giving just one number. Second, it only accounts for movements of the barycentre, which is not the only possible source of line distortion and line shift in a spectrograph. In fact, simulations show that even for circular fibers (which are known to have relatively poor scrambling gain) the contribution of imperfect scrambling on the barycentre shift is negligible (see Allington-Smith et al., 2012). In reality barycentric shifts are still measured due to inhomogeneities of the fiber surface, due to illumination dependent aberrations of the optics used for investigating the NF and due to an inhomogeneous sensitivity of the detector. All these effects are also present in a spectrograph, which means that by looking at the barycentric shift solely the effect of imperfect scrambling can be underestimated. On the other hand, the barycentric shift can easily be converted to a radial velocity error, whereas other measurements of the inhomogeneity of the NF such as RMS values or higher image moments do not have a direct relation to a RV error and are therefore only useful for relative comparisons of different fibers or scrambling methods.

4. DATA ANALYSIS AND RESULTS

4.1 Scrambling

The NF image sequence is analyzed using a pipeline written in python. After dark subtraction for each image a mask is created by blurring and thresholding the image. The mask covers the fiber image plus a small margin in order to make sure that the whole NF of the fiber is analysed. This method has two advantages compared to a simple weighted mean of the whole detector. First, noise from outside the region of interest is efficiently suppressed. Noise from pixels far from the barycenter can massively distort the results, especially when calculating higher image moments. Second, by analyzing the mask position one has a good indicator of how stable the setup was during the measurement. Ideally, the image of the NF will not stay at the exact same position, due to mechanical and thermal instabilities of the setup. In principle subtracting the mask position from the measured barycenters would correct for these movements of the fiber, but it is has to be done very carefully, as non-linearities and inhomogeneities might lead to ambiguous results. Fig. 4 shows the barycentric movement for different kinds of fibers. The plot style was adapted from Feger et al. (2012). There is clear improvement in the stability when using non-circular symmetric fibers. The shift of the barycenter of the output is reduced by a factor of almost 20 when using the circular-octagonal link. The RMS shift of the barycenters is about $0.16 \cdot d/1000$, which is $16\ \text{nm}$ or $\sim 1.2\ \text{ms}^{-1}$. The SG exceeds 1000, which was the requirement for CARMENES, except for the very smallest spot displacements (see lower right of Fig.4). Due to the definition of the scrambling gain systematic errors affect the result most for small displacements. This manifests in the small horizontal distance between the regions indicating different SG in Fig.4. Therefore, the lower SG at these positions is not considered to be problematic.

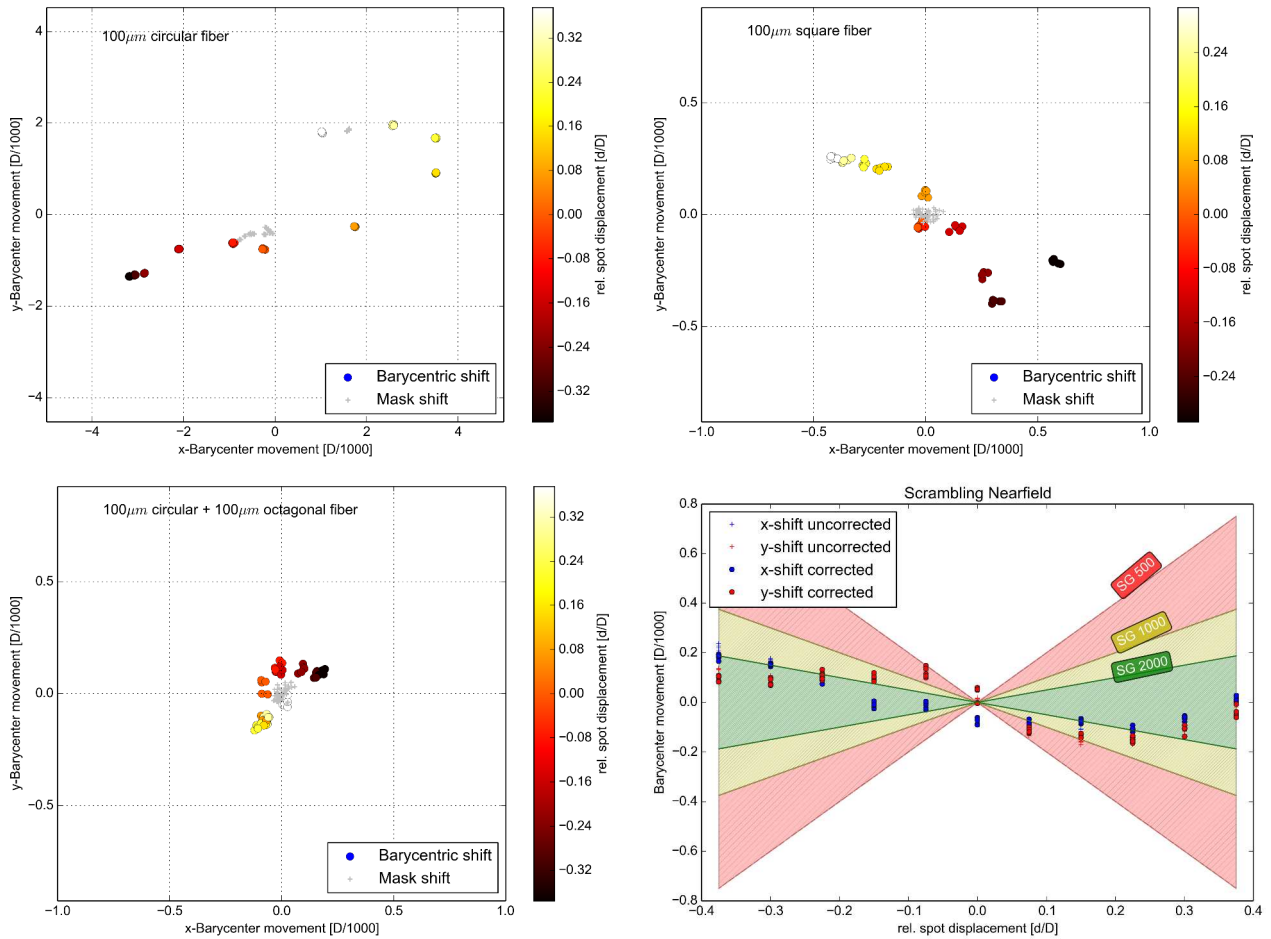


Figure 4. Barycentric movement of the fiber output for different spot displacements at the fiber entrance. Top left: 100 μm Circular Fiber (note different scaling) Top right: 100 μm Square Fiber, Bottom left: 100 μm Circular Fiber + Octagonal Fiber, Bottom right: 1D version also showing regions indicating different levels of SG as defined in Eq. 1

4.2 Farfield effects

The impact of a varying far-field on radial velocity precision is investigated by raytracing methods. For a number of wavelengths spot diagrams on the CCD are created while saving the intersection coordinates of each ray with the pupil plane of the spectrograph. For each ray of the spot diagram its pupil coordinate is known. This information allows one to determine the barycenter by calculating a weighted mean of all ray positions for different pupil illuminations. It has been made sure that the procedure is numerically stable, by comparing the results obtained with increasing number of sampling rays in the pupil plane. Different FF illumination therefore corresponds to a different weighting of the rays. Extreme cases like D-shaped apertures with different orientation can easily cause shifts in the order of several tens of meters per second. Although these cases are not realistic for normal telescope operation it illustrates how important the FF illumination is for the stability of the spectrograph. In order to get estimates on the RV errors for more realistic FF variations images of the FF for different coupling conditions have been taken in the lab. Slight defocus as well as various spot displacements at the fiber entrance have been used to generate a series of FF images. Fig.5 shows a typical FF of the circular-octagonal link as well as cross-sections of the FF for different fiber types. How a varying FF caused by spot

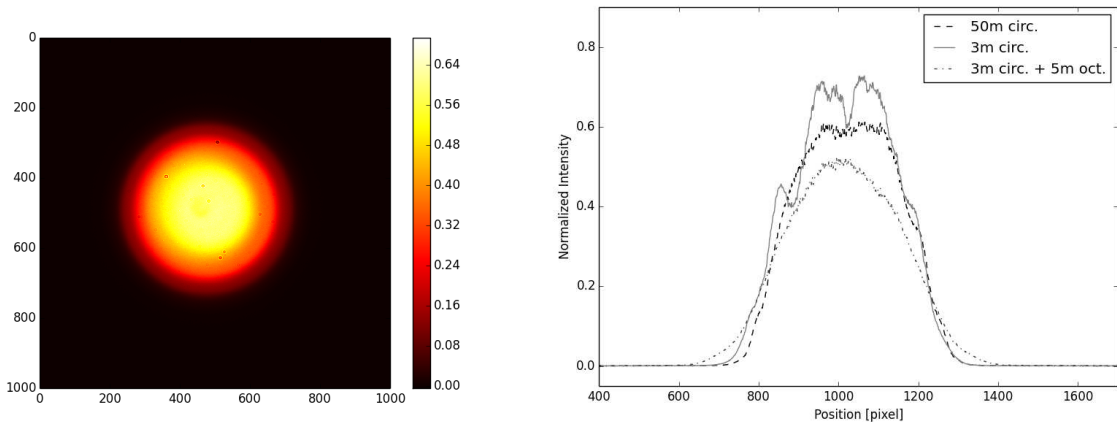


Figure 5. A typical FF image of the circular-octagonal fiber link (left). Compared to a single fiber, there are no irregular structures visible any more, to the cost of a higher FRD which manifests in faint wings on the outer part of the FF (right). Here the fiber was fed with a fairly slow beam ($\sim f/6$) to make the FRD easier to see.

displacement affects the barycenters of the spots can be seen in Fig.4.2 for the VIS and in Fig.4.2 for the NIR channel of CARMENES. Generally it can be seen that the effects of a varying FF on the stability are larger where optical aberrations are more prominent (i.e. in the corners of the detectors). In other words, the larger the spots are the more sensitive they are to illumination effects, which is intuitively plausible. Having a good control over optical aberrations is therefore very important for instrument stability. It can also be seen that the effects are mostly symmetric across the CCD. Averaging over many lines along one echelle order will therefore help to cancel out illumination effect. Again, this is a direct consequence of the symmetry of optical aberrations. The total shift for a single line caused by typical changes of the FF is below 1 m s^{-1} . However, it is difficult to predict how the FF varies on a real telescope over a longer period of time. Guiding, focussing and seeing have an impact on the exact shape of the FF. On-sky tests are planned in order to get more realistic data. Nevertheless it is instructive to perform these simulations to get a better understanding of the impact of optical aberrations on spectrograph stability. Another consequence of the described results affects the fiber coupling technique. There seems to be no agreement in the literature on whether feeding the pupil of the telescope or feeding the image of the telescope is superior in terms of spectrograph stability. At least in the case when no optical double scrambler is used but solely non-circular fibers (or a combination of fibers with different shapes), a telecentric feeding optic is clearly the best choice. While the fibers will efficiently stabilize the NF, the FF does not get much further stabilized. This means that the most dominant error sources, guiding errors and seeing variations are efficiently suppressed by the fiberlink, while the telescope pupil, which is known to be much more stable than the image will only gain a further stabilization due to smoothing caused by FRD.

For CARMENES the fibers are fed with $f/3.9$ at the telescope using a telecentric F/N system. The spectrograph

optics accept f/3.5, allowing for FRD. The prototype of the fiberlink showed a loss due to FRD of less than 3% for an f/3.5 output beam (and $\sim 8.5\%$ for an f/3.9 output beam).

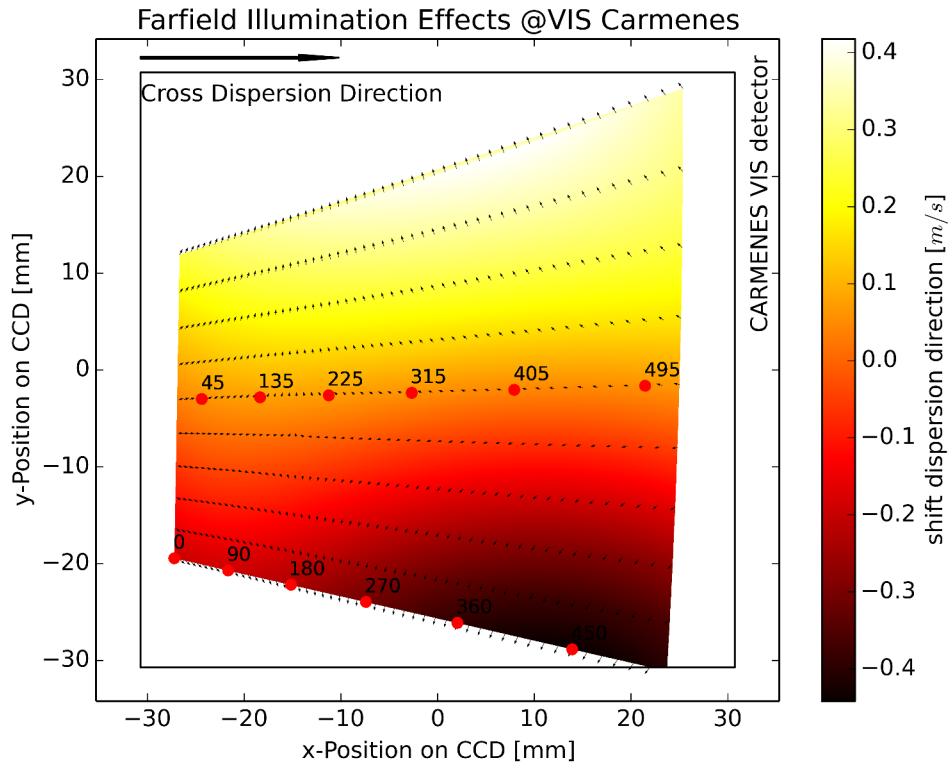


Figure 6. Two FF images are recorded in the lab with different coupling conditions, as they are expected to occur at the telescope. The image intensities are used as relative weights of each ray depending on its pupil coordinate. Calculating the weighted mean for both illuminations gives an estimate on how barycenters of a spectral line shift. In most cases the errors show a symmetry with respect to the centre of the echelle order.

4.3 Model effects

The limited number of modes supported by an optical fiber leads to an additional noise contribution in fiber coupled spectrographs. Radial velocity precision as well as the achievable signal-to-noise-ratio (SNR) is influenced by the illumination variations due to interference effects on the output of the fiber. Modal noise limits the SNR to

$$SNR = \frac{\rho}{\nu} \cdot \sqrt{\frac{M+1}{1-\rho^2}}, \quad (2)$$

where M denotes the number of supported modes, ν is the Michelson contrast of the speckle pattern and ρ^2 is the fraction of light reaching the detector (Goodman and Rawson, 1981; Lemke et al., 2011). Inhomogeneities of the grating and other sources of light loss entail that for any realistic spectrograph ρ^2 is smaller than unity. The number of modes M is given by fiber size, wavelength and coupling conditions and is therefore a fixed number for a spectrograph system. To keep ρ^2 as large as possible, overfilling of any spectrograph optics (including artificial slits after the fiber) must be avoided. The speckle contrast ν is the only variable left which can be manipulated to increase the SNR limit. Astronomical integration times are usually of the order of a few seconds to several minutes. The speckle contrast can therefore be reduced by inducing changes of the exact speckle pattern within this timeframe. Agitating the fiber is the simplest way to do so. Using piezo elements allows for well defined stretching or twisting of the fiber, but it requires access to the bare fiber (see Chen et al., 2006). Mahadevan

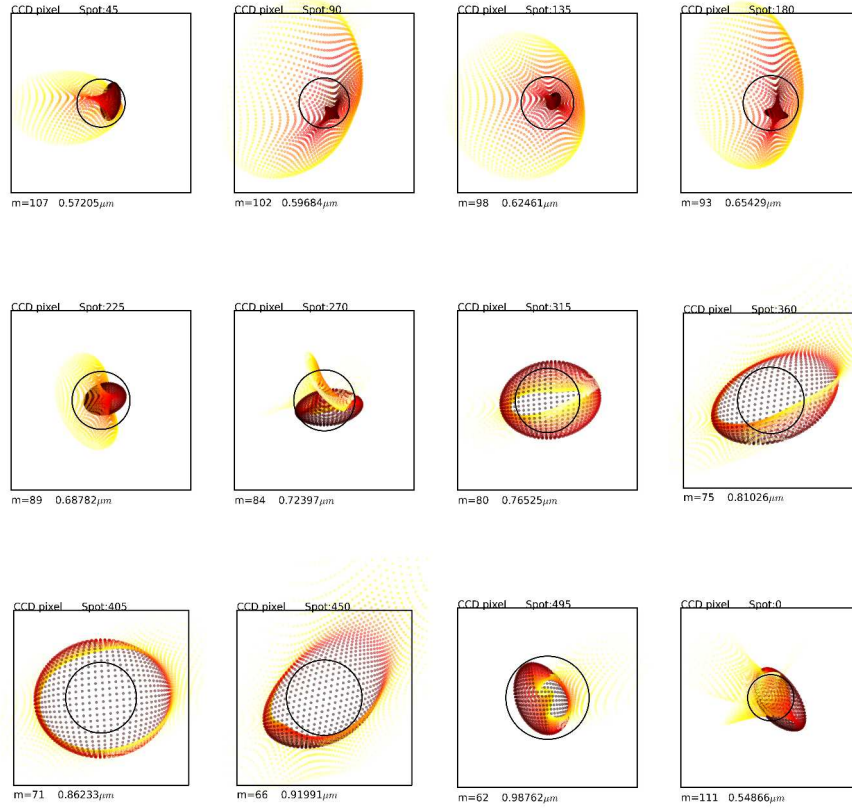


Figure 7. Spot diagrams of different spots across CCD of the VIS channel of CARMENES. The color is indicating the relative weight of each ray. The weights are extracted from FF images like Fig.5.

et al. (2014) recently developed a very effective method to minimize speckle contrast for the calibration light by using an integrating sphere combined with a dynamical diffuser. Due to the light loss of this solution it is not applicable for fibers transporting stellar light. Different ways of agitating these fibers have been tested in order to find a way to reduce the speckle contrast. These methods have been compared by calculating the Michelson contrast of the speckle pattern in the NF of the fiber:

$$\nu = \frac{I_{max} - I_{min}}{I_{max} + I_{min}} \quad (3)$$

A green laser is fed into a single mode fiber and re-imaged 1 to 1 to the fiber under investigation (a 100 μm circular fiber and a 67 μm octagonal fiber). Under this kind of illumination only a small number of modes is excited. This is done to simulate the lower number of modes available in the 100 μm fiber in the H-band, which could not be tested directly due to the lack of an appropriate detector. For analysis only an inner region of the recorded NF is used for calculating ν , because it is very difficult to determine the exact border of the fiber. The region of analysis has to be large enough to provide good statistics. As long as this criterion is fulfilled the contrast does not significantly depend on the exact region size any more. Before extracting the contrast value, dark subtraction and flatfielding is performed. The flatfield is created by illuminating the fiber with white light and agitating it. For the circular fiber flatfielding was necessary to cancel out the artificial increase of the speckle contrast due to the inhomogeneous illumination. Figure 9 shows speckle patterns and corresponding contrast values for different methods of agitation. As expected, the contrast for a non-agitated fiber is near unity (0.97). A gentle and regular movement of the fiber already reduces the contrast by a factor of ~ 2.5 . McCoy et al. (2012) has already shown that hand agitation is quite effective in reducing modal noise. We achieved similar

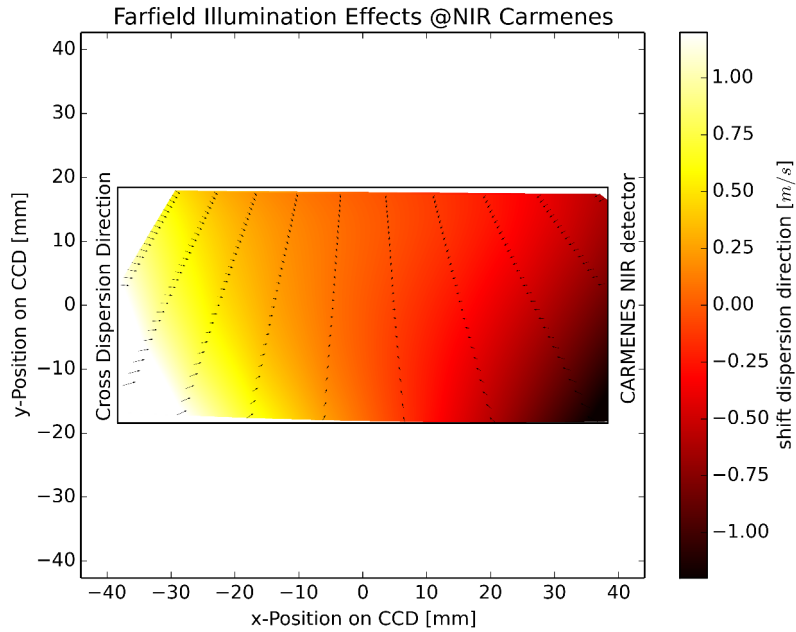


Figure 8. Shifts of the spectral lines due to typical FF illumination effects in the NIR channel of CARMENES

performance by the use of two subsequent mechanical agitators (wiper motors). Although this solution does not seem very elegant, it achieves a contrast reduction by a factor of ~ 4.5 , the same as what we reached by agitating the fiber by hand. On the other hand it is very easy to implement and maintain, cheap and robust. We also tested other methods, including low amplitude modulation of the bare fiber with frequencies of 20 Hz to 120 Hz and ultrasonic transducers. Although these methods work as well, the handling of bare fibers, especially in the case of a mechanical failure of the agitation device is delicate. Also, by holding bare fibers, additional FRD is easily introduced due to external stress. Our device does not perform a chaotic movement as suggested by Grupp (2003), however as the resulting speckle contrast is as low as in the case of non-regular hand agitation, we believe that a chaotic movement is not essential as long as the amplitude is high enough. Our tests also showed that if a double scrambler is used, the fiber after the bulk optics should be agitated. This might be a problem if the second fiber is completely within the tank (like for HARPS), where any moving parts are unwanted. Agitating only the first fiber has a significantly lower efficiency in speckle contrast reduction.

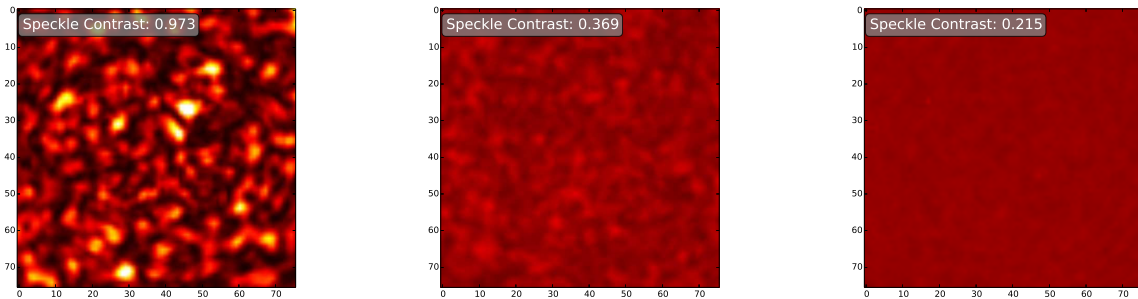


Figure 9. Speckle patterns and contrast values for different kind of fiber agitation. Left: no agitation. Middle: gentle regular mechanical movement. Right: two subsequent mechanical agitators with moderate agitation.

5. OUTLOOK AND CONCLUSION

Modern high-resolution spectrographs for precise radial velocity measurements demand a stable illumination of their slit. In general this always requires a trade-off between efficiency and stability. Non-circular fibers are known to provide very good image stability in the NF, which is supported by our measurements. A combination of a circular and octagonal fiber provides excellent scrambling while also efficiently removing structures in the FF. Variations in the FF of the fiber result in varying illumination of the spectrograph optics, therefore the optics have to be taken into account when investigating the impact on radial velocity precision. The simulations we performed allow for a prediction of the radial velocity shift for different FF illuminations. The results indicate that the 1 m s^{-1} precision goal of CARMENES can be reached with the combined circular, octagonal fiber link. The throughput is expected to be 15 % to 25 % higher than for an optical double scrambler.

ACKNOWLEDGMENTS

The authors thank Andreas Kelz, Roger Haynes, Dionne Haynes and others from the AIP and innoFSpec in Potsdam for letting us use their fiber preparation facilities and providing helpful advice. We also thank Rosalind Skelton and Christoph Bergmann for their help with the manuscript.

References

- Allington-Smith, J., Murray, G., and Lemke, U. (2012). Simulation of complex phenomena in optical fibres. *Monthly Notices of the Royal Astronomical Society*, 427:919–933.
- Avila, G. (1988). Tests of optical fibres for astronomical instrumentation at ESO. In Barden, S. C., editor, *Fiber Optics in Astronomy*, volume 3 of *Astronomical Society of the Pacific Conference Series*, pages 63–73.
- Bouchy, F., Díaz, R. F., Hébrard, G., Arnold, L., Boisse, I., Delfosse, X., Perruchot, S., and Santerne, A. (2013). SOPHIE+: First results of an octagonal-section fiber for high-precision radial velocity measurements. *Astronomy & Astrophysics*, 549:A49.
- Chen, C.-H., Reynolds, R. O., and Kost, A. (2006). Origin of spectral modal noise in fiber-coupled spectrographs. *Applied Optics*, 45:519–527.
- Feger, T., Brucalassi, A., Grupp, F. U., Lang-Bardl, F., Holzwarth, R., Hopp, U., and Bender, R. (2012). A testbed for simultaneous measurement of fiber near and far-field for the evaluation of fiber scrambling properties. In *Society of Photo-Optical Instrumentation Engineers (SPIE) Conference Series*, volume 8446 of *Society of Photo-Optical Instrumentation Engineers (SPIE) Conference Series*.
- Goodman, J. W. and Rawson, E. G. (1981). Statistics of modal noise in fibers - A case of constrained speckle. *Optics Letters*, 6:324–326.
- Grupp, F. (2003). The nature of the fiber noise with the FOCES spectrograph. Nature, modeling and a way to achieve $S/N \gtrsim 400$. *Astronomy & Astrophysics*, 412:897–902.
- Haynes, D. M., Withford, M. J., Dawes, J. M., Lawrence, J. S., and Haynes, R. (2011). Relative contributions of scattering, diffraction and modal diffusion to focal ratio degradation in optical fibres. *Monthly Notices of the Royal Astronomical Society*, 414(1):253263.
- Lemke, U., Corbett, J., Allington-Smith, J., and Murray, G. (2011). Modal noise prediction in fibre spectroscopy - I. Visibility and the coherent model. *Monthly Notices of the Royal Astronomical Society*, 417:689–697.
- Mahadevan, S., Halverson, S., Ramsey, L., and Venditti, N. (2014). Suppression of Fiber Modal Noise Induced Radial Velocity Errors for Bright Emission-line Calibration Sources. *The Astrophysical Journal*, 786:18.
- McCoy, K. S., Ramsey, L., Mahadevan, S., Halverson, S., and Redman, S. L. (2012). Optical fiber modal noise in the 0.8 to 1.5 micron region and implications for near infrared precision radial velocity measurements. In *Society of Photo-Optical Instrumentation Engineers (SPIE) Conference Series*, volume 8446 of *Society of Photo-Optical Instrumentation Engineers (SPIE) Conference Series*.

Murphy, J. D., MacQueen, P. J., Hill, G. J., Grupp, F., Kelz, A., Palunas, P., Roth, M., and Fry, A. (2008). Focal ratio degradation and transmission in VIRUS-P optical fibers. In *Society of Photo-Optical Instrumentation Engineers (SPIE) Conference Series*, volume 7018 of *Society of Photo-Optical Instrumentation Engineers (SPIE) Conference Series*.

Wang, R., Yan, Y., Liu, Y., Zhang, H., and Sun, W. (2013). The influence on frd with different encircled energy. In *Optoelectronics and Microelectronics (ICOM), 2013 International Conference on*, pages 180–182.